

# PSEUDOGAP VALUE IN THE ENERGY SPECTRUM OF LaOFeAs: A FIXED SPIN MOMENT TREATMENT

*M. A. Korotin\*, S. V. Streltsov, A. O. Shorikov, V. I. Anisimov*

*Institute of Metal Physics, Russian Academy of Sciences  
620041, Yekaterinburg, Russia*

Received May 23, 2008

The experimental data currently available in the literature on the paramagnetic–spin density wave transition in nonsuperconducting LaOFeAs are discussed. In particular, we note that a relative decrease in the density of states on the Fermi level and a pseudogap formation occur upon a spin density wave transition. The values of these quantities are not properly described in the framework of the density functional theory. The agreement with experimental estimations becomes more accurate with the use of a fixed spin moment procedure when the iron spin moment is set to the experimental value. Strong electron correlations that are not included into the present calculation scheme may lead both to a decrease in the spin moment and to a renormalization of the energy spectrum in the vicinity of the Fermi level for correct description of the discussed characteristics.

PACS: 71.15.Mb, 74.25.Jb

Stimulated by the discovery of a new class of high- $T_c$  superconductors based on the LaOFeAs compound [1], numerous investigations of the electronic and magnetic structure of this nonsuperconducting parent compound were performed in the framework of the density functional theory (DFT) [2–6]. These calculations were successful in predicting not only the magnetic instability [2, 5] but also an exact type of the magnetic structure of LaOFeAs [4, 7].

The calculated iron magnetic moment is close to  $2\mu_B$  [6, 8]. But experiments indicate a much smaller value. Powder neutron diffraction measurements [9] give  $0.36(5)\mu_B$ . Local probe measurements of magnetic properties of LaOFeAs such as  $^{57}\text{Fe}$  Mössbauer spectroscopy [10] together with muon spin relaxation [11] indicate the respective values  $\sim 0.35\mu_B$  and  $0.25(5)\mu_B$ .

The situation when DFT calculations predict larger spin magnetic moment in comparison with the experimental one is rare and known only for few systems (e.g., MnSi and  $\text{ZrZn}_2$ ). The inconsistency between experimental and calculated magnetic moments in these materials may be ascribed to spin fluctuations that lead to the suppression of magnetic moment [12]. Nevertheless, LaOFeAs is an outstanding compound even among these systems because the ratio  $\mu_{calc}/\mu_{exp}$  is extraordi-

nary large, approximately equal to 6; more importantly, Fe ions in the simple atomic picture are expected to have  $S = 2$ , which cannot be easily suppressed by any quantum fluctuations.

The other known experimental parameters that can be compared with their theoretical values are the specific heat coefficient  $\gamma$  related to the density of states (DOS) on the Fermi level  $N(E_F)$  as  $\gamma = (\pi^2/3)k_B^2 N(E_F)$  and the Pauli susceptibility  $\chi = \mu_B^2 N(E_F)$ . The specific heat coefficient can be extracted from the low-temperature behavior of the heat capacity. Unfortunately, this parameter is ill-defined experimentally, i.e., strongly depends on the temperature range used in the fitting procedure. It was estimated by different groups to be  $3.7 \text{ mJ}/(\text{mol}\cdot\text{K}^2)$  [7],  $0.9 \text{ mJ}/(\text{mol}\cdot\text{K}^2)$  [13], and  $0.69 \text{ mJ}/(\text{mol}\cdot\text{K}^2)$  [14]. But  $\gamma$  obtained in nonmagnetic DFT calculations [2, 5] overestimates the largest experimental value by almost two times. The results of magnetic calculations for the real striped antiferromagnetic structure [8] improve the situation. They are close to the intermediate experimental  $\gamma$  value. However, this coincidence may be considered accidental because the electronic structure of this antiferromagnetic solution corresponds to a large iron magnetic moment. The susceptibility calculated in the framework of the nonmagnetic DFT is  $8.5 \cdot 10^{-5} \text{ emu/mol}$  [2]. At the same time, the flat region

\*E-mail: michael.korotin@gmail.com

of the experimental susceptibility curve has the value about  $50 \cdot 10^{-5}$  emu/mol [1, 15], 6 times larger than the calculated one.

There is an experimental indication of the formation of a partial energy gap (or pseudogap) around the Fermi level, which removes parts of the DOS or few bands from the Fermi energy at the phase transition from the paramagnetic to the spin density wave (SDW) state. Direct experimental estimations of the pseudogap  $E_{pg}$  are based on the results of reflectivity measurements [7]. The pseudogap associated with a decrease in optical absorption spectra observed at different temperatures corresponding to paramagnetic and SDW states is in the range  $150\text{--}350$  cm $^{-1}$  (19–43 meV). The value of the pseudogap due to SDW formation evaluated from thermal transport experiments is equal to 210 K [13], which corresponds to 18 meV. Results of a temperature-dependent angle-integrated laser photoemission study for a fluorine-doped compound indicate a pseudogap about 100 meV [16], whereas high-resolution photoemission spectroscopy [17] gives the above- $T_c$  pseudogap value 15–20 meV.

The evaluation of the relative reduction of the DOS in the vicinity of the Fermi energy due to the formation of such a pseudogap is a less direct procedure. Based on the results of susceptibility measurements [15], one can deduce from the values of Pauli-like susceptibility curves at high and low temperatures that the change in the  $N(E_F)$  does not exceed 20%. The same value of approximately 20% may be extracted from the conductivity curves in Ref. [7], keeping in mind that conductivity is proportional to  $N^2(E)$  in the proximity of  $E_F$ . Analysis of the specific heat at various temperatures [13] suggests a 70% reduction of  $N(E)$  around  $E_F$  under the paramagnetic–SDW transition.

Thus, for LaOFeAs, we can assume that there is a decrease in the DOS near the Fermi energy of tens percent under the paramagnetic–SDW transition, which corresponds to the formation of a 20–100 meV pseudogap. The SDW state is characterized by the iron spin magnetic moment  $0.2\text{--}0.4\mu_B$ , the specific heat coefficient 1–4 mJ/(mol·K $^2$ ), and the susceptibility coefficient approximately equal to  $50 \cdot 10^{-5}$  emu/mol. Conventional DFT calculations (both nonmagnetic and antiferromagnetic) fail to correctly describe these quantities.

In the present paper, we show that fixed spin moment DFT calculations with the magnetic moment fixed at the experimental value can significantly improve an agreement with the experiments with regard to the specific heat and pseudogap values and the relative decrease in the  $N(E_F)$  value.

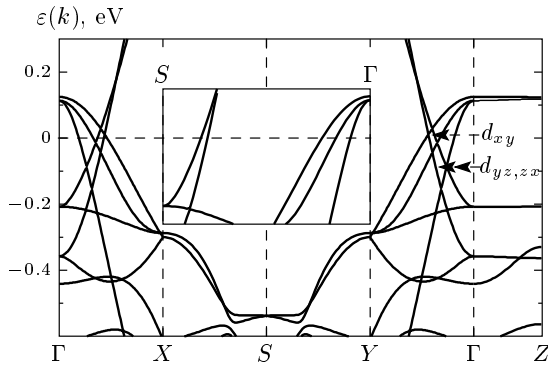
The calculations were performed in the framework of the method of tight-binding linear muffin-tin orbitals (TB LMTO) [18] using the generalized gradient approximation (GGA), where the exchange potential was taken in the Perdew–Wang form [19]. Experimentally determined [9] structure parameters and atomic positions for tetragonal phase and collinear striped antiferromagnetic order of Fe ions in layer were used. For simplicity, we assumed a ferromagnetic interlayer interaction due to a negligible influence of the antiparallel alignment of spins between different FeAs layers. The La(6s,6p,5d,4f), Fe(4s,4p,3d), O(3s,2p,3d), and As(4s,4p,4d) orbitals were included into the basis set. The integration in the course of self-consistency iterations was performed over a mesh of  $18 \times 18 \times 12$   $\mathbf{k}$ -points in the irreducible part of the Brillouin zone. We checked that this number of  $\mathbf{k}$ -points suffices for the precise calculation of the Fermi level position  $E_F$  and the value of the density of states at the Fermi level  $N(E_F)$ . A fine mesh is important due to the nesting bands near  $E_F$ . Calculations were performed in a  $\sqrt{2}a \times \sqrt{2}a \times c$  (four formula units) unit cell appropriate for description of a striped antiferromagnetic state. Crystallographic  $x$  and  $y$  axes were directed from iron to its nearest iron neighbors and ferromagnetic chains were running along the  $x$  direction.

Figure 1 demonstrates the results of nonmagnetic calculations. The band structure agrees with that obtained previously [8]. The Fe bands mainly of a  $t_{2g}$  origin cross the Fermi level. We note the two-dimensional character of the band structure and clear signs of Fermi surface nesting in  $\Gamma$ – $X$  and  $Y$ – $\Gamma$  directions.

The nesting effect is usually illustrated in the figure of the Fermi surface. To reveal nesting in the simple band structure graph, we plot it along the  $S$ – $\Gamma$  line for the conventional  $a \times a \times c$  unit cell; the result is given in the inset to Fig. 1. This  $S$ – $\Gamma$  direction corresponds to the  $Y$ – $\Gamma$  (or  $X$ – $\Gamma$ ) line for the enlarged  $\sqrt{2}a \times \sqrt{2}a \times c$  unit cell. When the unit cell is doubled, the left half of the inset folds to the right half. The crossing of the folded bands occurs just on the Fermi level.

The specific heat and susceptibility coefficients recalculated from  $N(E_F)$  obtained in the nonmagnetic DFT approach are  $\gamma_{NM} = 5.3$  mJ/(mol·K $^2$ ) and  $\chi_{NM} = 7.2 \cdot 10^{-5}$  emu/mol. That agrees with the values calculated before.

The total energy difference between nonmagnetic and antiferromagnetic (which is energetically more favored) states is 116 meV/(Fe atom), which is in good agreement with the result in Ref. [8]. A substantial energy gap between different magnetic solutions together with the large magnetic moment (see below) shifts the



**Fig. 1.** Band structure of LaOFeAs obtained from a nonmagnetic calculation in the Brillouin zone corresponding to the enlarged  $(\sqrt{2}a \times \sqrt{2}a \times c)$  unit cell. Inset: band structure along the  $S$ - $\Gamma$  line for the conventional  $(a \times a \times c)$  unit cell. The Fermi energy is zero. For the bands crossing the Fermi level, orbital projections are marked

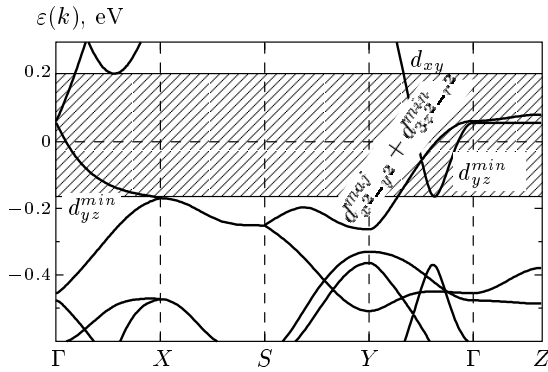


**Fig. 2.** Band structure of LaOFeAs for a striped antiferromagnetic state. The pseudogap energy region is shown by a hatched stripe. The Fermi energy is zero. For the bands crossing the Fermi level, orbital projections are marked. Superscripts indicate majority (*maj*) and minority (*min*) spin projections. There are contributions from both majority and minority states to the band  $d_{xy}$

system away from the quantum critical point, where spin fluctuations may play an important role. The band structure for the striped antiferromagnetic state is shown in Fig. 2. It differs essentially from the nonmagnetic picture. In particular, in the vicinity of the Fermi level in the  $\Gamma$ - $X$  direction, there is only one band of the  $d_{yz}^\downarrow$  character. The other four bands are moved away from the Fermi level due to the Stoner splitting. In the  $Y$ - $\Gamma$  direction, three bands remain. Two of them ( $d_{xy}$  and  $d_{yz}$ ) have the same origin as in the nonmag-

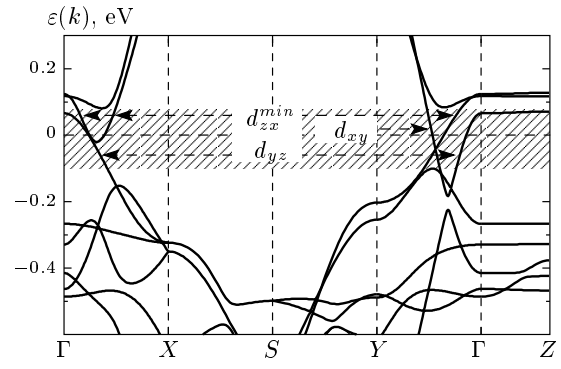


**Fig. 3.** Band structure of LaOFeAs for the striped antiferromagnetic state with the fixed spin moment value  $0.36\mu_B$ . See also the caption to Fig. 2

netic state and the third band originates from  $d_{x^2-y^2}^\uparrow$  and  $d_{3z^2-r^2}^\downarrow$  orbitals, which were completely occupied in the nonmagnetic case.

The pseudogap can be defined as the energy region around the Fermi level where the number of bands in Fig. 2 is essentially smaller than in Fig. 1. It is natural to define it to lie between the maximum of the parabola at the  $X$   $k$ -point and the minimum of a higher-lying parabola in the  $\Gamma$ - $X$  direction (see the hatched stripe in Fig. 2). The pseudogap defined in this way is estimated to be 380 meV, which is much larger than experimental expectations.

The calculated iron magnetic moment is equal to  $1.77\mu_B$  and the specific heat coefficient  $\gamma_{MAG} = 0.99$  mJ/(mol·K<sup>2</sup>). This agrees with the experimental estimations of  $\gamma$  [13]. However, in going from the nonmagnetic to the antiferromagnetic phase, the calculated value of  $N(E_F)$  changes by a factor of 6 (600% instead of tens percent).

This inconsistency in the values of magnetic moment and the width of the pseudogap, and too drastic a change in  $N(E_F)$  in going from the paramagnetic to the magnetic state demands an explanation. Below, using the fixed spin moment procedure, we simulate the experimental value of the magnetic moment and investigate how  $N(E_F)$  and the pseudogap width change upon a decrease in the spin moment value.

The band structure corresponding to the fixed spin moment value  $0.36\mu_B$  is presented in Fig. 3. It looks very similar to the nonmagnetic picture. A remarkable difference occurs along the  $\Gamma$ - $X$  direction:  $d_{xy}$  and  $d_{zx}$  bands are spin-split and the first of them is removed from the vicinity of the Fermi level, whereas  $d_{yz}^\downarrow$  is still crossing  $E_F$ . There is no dramatic rearrangement of bands along the  $Y$ - $\Gamma$  direction. We conclude that under the transition from the nonmagnetic to the mag-

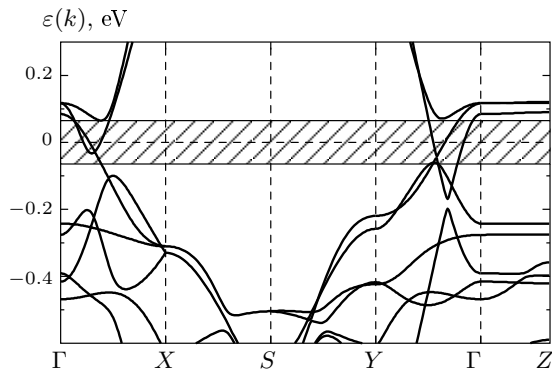


**Fig. 4.** Band structure of LaOFeAs for a striped anti-ferromagnetic state with the fixed spin moment value  $0.25\mu_B$ . See also the caption to Fig. 2

netic state, the first changes of the band structure occur along the  $\Gamma$ - $X$  line; then the bands along  $Y$ - $\Gamma$  are involved in the formation of magnetic moment.

The fixed spin moment calculation results in a significant increase in the specific heat coefficient, which is equal to  $\gamma_{FSM} = 2.0 \text{ mJ}/(\text{mol}\cdot\text{K}^2)$  in this case, in a good agreement with experiment. The pseudogap, which can now be defined as indicated by the hatched stripe in Fig. 3, decreases to 180 meV, which is still larger than the experimental value.

It is interesting to note that a further decrease in the magnetic moment in the fixed spin moment calculation (Fig. 4) leads to an even better agreement with experiment as regards the value of the pseudogap. For one of the reported values of  $\mu = 0.25\mu_B$ , it decreases to 130 meV. The specific heat parameter is calculated to be  $2.4 \text{ mJ}/(\text{mol}\cdot\text{K}^2)$ , and then the change in  $N(E_F)$  in nonmagnetic and magnetic states is only 55 %, in reasonable agreement with experimental estimations.

The semiempirical fixed spin moment approach demonstrates that the correspondence of experimentally known parameters of the electronic structure of LaOFeAs is essentially improved in comparison with the conventional magnetic calculations if the magnetic moment is kept at a low value near  $0.3\mu_B$  found in the experiment. However, even with the reduced spin moment value, the calculated pseudogap (130 meV) remains larger than the experimental one (20–40 meV).

In our opinion, an account for dynamical correlations, which certainly exist for the  $d$  shell of iron, may lead both to an essential reduction in the spin moment value and to a renormalization of the energy spectrum in the vicinity of the Fermi level for decreasing the pseudogap.

This work was supported by the Dynasty Foundation and the International Center for Fundamental Physics in Moscow, the Russian Foundation for Basic Research Grants RFFI 07-02-91567 and 07-02-00041, the Civil Research and Development Foundation, and the Russian Ministry of science and education Grant Y4-P-05-15, the Russian president grant for young scientists MK-1184.2007.2, and a grant of the Ural division of RAS for young scientists.

## REFERENCES

1. Y. Kamihara, T. Watanabe, M. Hirano et al., *J. Amer. Chem. Soc.* **130**, 3296 (2008).
2. D. J. Singh and M. H. Du, *Phys. Rev. Lett.* **100**, 237003 (2008).
3. C. Cao, P. J. Hirschfeld, and H.-P. Cheng, *Phys. Rev. B* **77**, 220506 (2008).
4. I. I. Mazin, D. J. Singh, M. D. Johannes et al., arXiv:0803.2740.
5. G. Xu, W. Ming, Y. Yao et al., *Europhys. Lett.* **82**, 67002 (2008).
6. F. Ma and Z.-Y. Lu, *Phys. Rev. B* **78**, 033111 (2008).
7. J. Dong, H. J. Zhang, G. Xu et al., *Europhys. Lett.* **83**, 27006 (2008).
8. Z. P. Yin, S. Lebègue, M. J. Han et al., *Phys. Rev. Lett.* **101**, 047001 (2008).
9. C. de la Cruz, Q. Huang, J. W. Lynn et al., *Nature* **453**, 899 (2008).
10. S. Kitao, Y. Kobayashi, S. Higashitaniguchi et al., arXiv:0805.0041.
11. H.-H. Klauss, H. Luetkens, R. Klingeler et al., arXiv:0805.0264.
12. I. I. Mazin, D. J. Singh, and A. Aguayo, in *Proceedings of the NATO ARW on Physics of Spin in Solids: Materials, Methods and Applications*, ed. by S. Halilov, Kluwer, Dordrecht (2003).
13. M. A. McGuire, A. D. Christianson, A. S. Sefat et al., arXiv:0804.0796.
14. G. Mu, X. Zhu, L. Fang et al., *Chinese Phys. Lett.* **25**, 2221 (2008).
15. T. Nomura, S. W. Kim, Y. Kamihara et al., arXiv:0804.3569.
16. Y. Ishida, T. Shimojima, K. Ishizaka et al., arXiv:0805.2647.
17. T. Sato, S. Souma, K. Nakayama et al., *J. Phys. Sec. Jpn.* **77**, 063708 (2008).
18. O. K. Andersen and O. Jepsen, *Phys. Rev. Lett.* **53**, 2571 (1984).
19. J. P. Perdew and Y. Wang, *Phys. Rev. B* **45**, 13244 (1992).